Proceedings of the 17th World Congress
The International Federation of Automatic Control
Seoul, Korea, July 6-11, 2008

Digital Filters for Gain Stabilization of Flexible Vehicle Dynamics

Raza Samar

Centre for Control and Instrumentation, National Engineering and Scientific Commission, Islamabad 44000, Pakistan.
(e-mail: raza@mail.comsats.net.pk).

Abstract: The necessity of having low-cost aerospace vehicles with short development times means that control designers need to work with simplified and approximate dynamic models. Aerospace vehicles typically being light and slender, exhibit body bending and flexibility effects at relatively lower frequencies. It may not be possible or practical in every case to carry out detailed test and analyses exercises to determine the structural dynamic characteristics of a vehicle. So, body bending shapes and slopes may not be precisely known; the mode frequencies can however be roughly estimated through simplified analysis. Here it will be assumed that the flexible mode frequencies are approximately known, and are sufficiently high so that gain stabilization is possible. This paper discusses different digital filters for gain stabilization of flexible vehicles, and elaborates their advantages and drawbacks. Various filters are compared; Butterworth, Bessel, Chebychev, Elliptical and simple quadratic filters of various orders are discussed. The filter selection is based on having desirable magnitude attenuation characteristics while at the same time leading to minimum phase lag near the closed-loop bandwidth. The filter design and selection process is illustrated by an example of a sounding rocket stabilization problem. Two flights of the vehicle have been conducted, the first with no consideration of the body-bending dynamics and hence no filters. Serious problems were observed, hence Elliptic filters were used to provide gain stabilization in the second flight. Flight test results are presented and discussed.

Keywords: Aerospace control; Gain stabilization; Flexible dynamics; Digital filters; Sounding rockets

1. INTRODUCTION

There has been a tremendous growth of low-cost unmanned airborne vehicle applications in the recent past. The applications are diverse, ranging from surveillance to scientific research. Similarly, space and upper atmosphere missions for scientific measurements have also increased with the emphasis lying on being low-cost. Sounding rockets are routinely used for modeling the upper atmosphere of the earth; these have reasonably tight guidance and control requirements so as to follow the desired trajectory closely, while at the same time development time and cost is to be kept at a minimum.

The necessity of having low-cost aerospace vehicles with short development times means that control designers need to work with simplified and approximate dynamic models. Aerospace vehicles typically being light and slender, exhibit body bending and flexibility effects at relatively lower frequencies. The control or autopilot sensors can pick up these bending modes and the control loop can oscillate or resonate at these frequencies resulting in fatal accidents (Noll *et al.* [1970], Noll and Zvara [1971] and Chang *et al.* [2000]). The vehicle control system or autopilot can be designed to stabilize and/or filter out the bending modes. Control system design therefore requires the investigation of the dynamic characteristics of the entire vehicle including all significant vibration modes (Livet *et al.* [1995], Idan *et al.* [1999], Dotson *et al.* [1998] and Blakelock [1991]). However, it is not possible or practical in every case to carry out a detailed test and analysis exercise to determine the structural dynamic characteristics of a vehicle, this being especially true for low-budget projects with tight development schedules. Body bending shapes and slopes therefore, may not be precisely known for many vehicles for use in controller design. The mode frequencies can however be roughly estimated through simplified analyses. In this paper, it will be assumed that the flexible mode frequencies are approximately known, and are sufficiently high so that gain stabilization is possible. This paper discusses different digital filters (some useful references are Mathworks [1999,2001], Antoniou [1993], Mitra [1998] and Oppenheim [1989]) that can be used for gain stabilization of flexible vehicles, and elaborates their advantages and drawbacks.

The fundamental concept presented is to use just the approximate mode frequency information to design digital filters that would allow subsequent controller design without consideration of the flexible modes, their shapes and slopes. Notch filters cannot be used because precise modal frequencies are not known. Hence low-pass filters must be employed. Various low-pass filters are compared. Butterworth, Bessel, Chebyshev, and Elliptic filters are discussed (see for example, Jackson [1996] and Chirlian [1994]). The filter selection is based on having desirable magnitude attenuation characteristics while at the same time leading to minimum phase lag near the closed-loop bandwidth. The filters are designed in the continuous domain and then discretized. The frequency response of the continuous and discrete filters is compared and the difference due to discretization is examined. The continuous domain (or analog) filters are re-synthesized to cater for changes in the

frequency response due to the discretization process. The filter design and selection process is illustrated by an example of a sounding rocket stabilization problem. The rocket is an experimental vehicle whose first flight was conducted with no consideration of the flexible dynamics. The results indicated the need to properly stabilize and/or filter the bending modes; Elliptic filters were therefore designed and implemented on the next flight. Results of the flight tests results are presented and discussed.

2. COMPARATIVE STUDY OF DIFFERENT FILTERS

A comparative study of different well-known filters is presented here. The only information for design of the gain stabilizing filter is that the first bending mode of the vehicle lies above 15 Hz. The requirement is to have a minimum of 40 dB attenuation at and above 15 Hz (94.25 rad/sec). Six filters are designed to meet these objectives. These are of 3rd order each. Their frequency response is shown in Figs. 1 and 2. In Fig. 1, the solid line is for the Butterworth filter, the dotted line for the Chebyshev Type I filter and the dashed line corresponds to the Elliptic or Cauer filter. Chebyshev Type I filters are equiripple in the passband and monotonic in the stopband (Mathworks [1999]). All three filters are analog (designed in the s-domain). The Butterworth and Chebyshev-I filters are quite close, however the phase lag for the Chebyshev-I filter is slightly better at lower frequencies (10~20 rad/sec). The Elliptic filter has steeper roll-off characteristics than the other two filters. The ripple in the passband and stopband is not critical for our application. However, the lesser phase lag at lower frequencies is favourable from the closed-loop stability viewpoint. The bandwidth of the closed loop system is expected to be around 10 rad/sec and hence better phase characteristics close to this frequency are important.

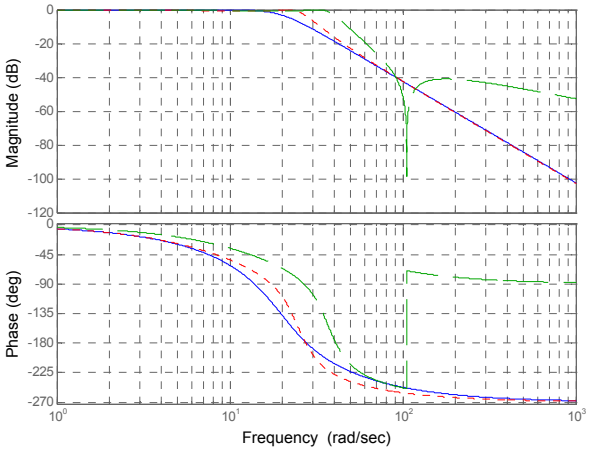

Fig. 1. Frequency response: Butterworth, Chebychev-I and Elliptic filters.

Three other filters are compared in Fig. 2. The solid line is for the Bessel 3rd order filter whereas the dashed line represents the Chebyshev Type II filter. Type II filters are monotonic in the passband and equiripple in the stopband (Mathworks [1999]). The dotted line is for the following filter:

$$X(s) = \frac{19.75^2 \times 20}{(s^2 + 2\times 0.325 \times 19.75 s + 19.75^2)(s+20)} \qquad (1)$$

The Chebyshev-II shows better phase characteristics at lower frequencies as compared to the other two filters.

The frequency responses of Chebyshev-II and Elliptic filters are very close to each other. The Elliptic filter is equiripple in both the passband and the stopband whereas the Chebyshev-II filter is monotonic in the passband. As a result the Elliptic filter displays slightly lesser phase lag at lower frequencies (10~20 rad/sec). The Elliptic filter is therefore selected for the gain stabilization problem.

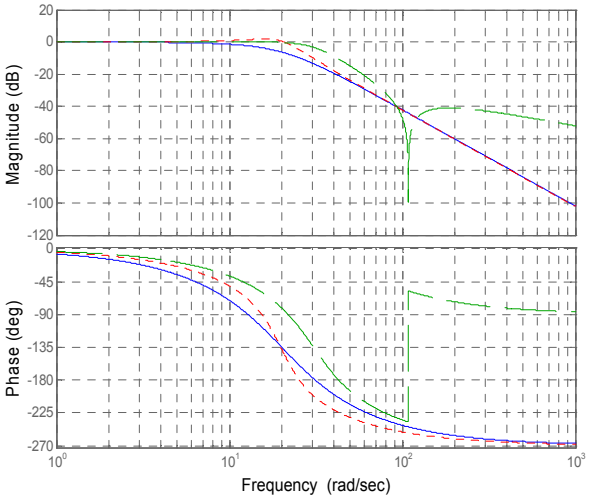

Fig. 2. Frequency response: Bessel, Chebychev-II and X(s) filters.

The pole-zero map of the Elliptic filter reveals that it has a pair of zeros on the imaginary axis. This is not desirable since numerical rounding errors can give rise to a non-minimum phase system. The zeros of the filter are moved slightly into the left-half plane without significantly affecting the filter frequency response. The frequency response of the original (solid line) and modified (dashed line) Elliptic filters is shown in Fig. 3. The modified filter has the zero pair shifted from $0 \pm 105.17j$ to $-1.0517 \pm 105.17j$. The modified filter will be discretized in the next section; the s-domain representation is given below:

$$H(s) = 2.3565 \frac{s^2 + 2.103s + 11060}{(s+19.18)(s^2 + 16.82s + 1359)}$$

3. EFFECTS OF DISCRETIZATION

The filters presented in the previous section are all analog 3rd order filters (designed in the s-domain). For implementation on an embedded computer, the discrete form is required. A

sample rate of 20 msec is chosen and discretization is performed using the Bilinear (Tustin's) approximation (Franklin *et al.* [1998]). The frequency response of the analog and discretized Elliptic filters is shown in Fig. 4. The solid line represents the analog filter response and the dashed line the discrete filter response.

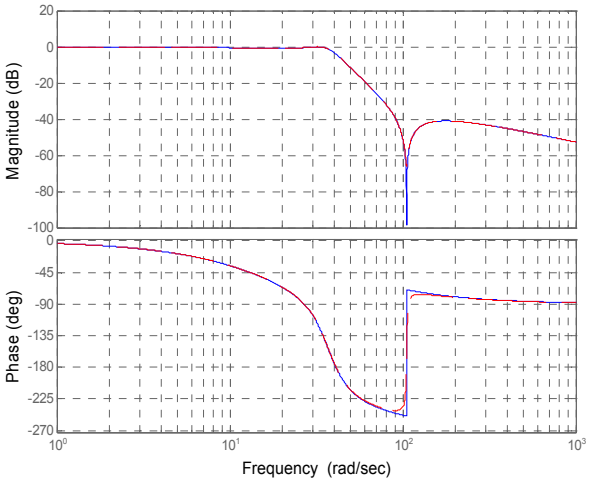

Fig. 3. Frequency Response: Original and modified Elliptic filters.

The effect of discretization is clearly seen. The frequency response of the filter is altered due to the discrete approximation. The -40 dB point is shifted from 14.48 Hz to 11.74 Hz. This shift is undesirable. The discrete filter is therefore adjusted so that the -40 dB point matches with the analog filter. The adjustment is done by a simple trial and error process of selecting the analog design parameters so that after discretization the desired frequency characteristics are achieved. The frequency response of the adjusted discrete filter (Fig. 5) reveals that the -40 dB point now matches with the original analog filter (solid line). It may be noted that the discrete filter (dashed line) is not the transformation of the analog filter (solid line) of Fig. 5, but of an adjusted analog filter so that the frequency response after discretization meets the requirement. The adjusted discrete filter is given below:

$$H(z) = 0.0557 \frac{(z+1)(z^2+0.7536z+1)}{(z-0.574)(z^2-0.966z+0.685)}$$

4. AN APPLICATION: SOUNDING ROCKET CONTROL

The application discussed below is that of a sounding rocket designed to explore the upper atmosphere. The rocket is long and slender and the only information available about its structural modes is that the first mode is greater than or equal to 15 Hz. Hence the filters discussed above are designed with this application in mind. The control system closed-loop simulation block diagram is shown in Fig. 6. The *Lateral Dynamics* block captures the non-linear equations of motion and the time-varying dynamics of the rocket as it flies through the lower atmosphere into the upper rarer atmosphere. v_g and p_g are gust disturbance inputs, F_{yc} and L_c are lateral control force and roll control moment, and F_{ye}, L_e and N_e are lateral disturbance force, and roll and yaw disturbing moments, respectively. The yaw angle *psi* and the lateral velocity and position V_i and y_i are used to close the loops. For the simulation results presented here, the lateral guidance gain *Lg_gain* is kept zero, thus essentially reducing the block diagram to an attitude control loop only. The block *Discrete Filter* implements the adjusted Elliptic filter discussed above and the *Discrete Controller* block implements an H_∞ controller designed using the loop-shaping design procedure of McFarlane and Glover [1990,1992].

The loop-shaping design procedure is intuitive in that it is based on the generalization of classical loop-shaping ideas. The open-loop plant, once given the desired loop-shape, is robustly stabilized against coprime factor uncertainty. The resulting controller has been shown to enjoy some favourable properties, such as no pole-zero cancellation occurs in the closed-loop system (except for a certain special class of plants), see Tsai *et al.* [1992]. In addition, the controllers thus designed have been successful in various applications; examples are those described by Samar *et al.* [1996], Smerlas *et al.* [2001] and Skogestad and Postlethwaite [2005]. The design starts with an evaluation of the frequency response of the plant model (which is a model of the rocket dynamics cascaded with the actuator and sensor transfer functions). The frequency response is then shaped by pre- and/or post-multiplication with weighting functions W_1 and W_2 to form the shaped plant W_2GW_1, G being the original plant model. Shaping is typically done so as to yield a high loop gain at low frequencies for good disturbance rejection and tracking, and a low gain at high frequencies for robustness and noise suppression. The shaped plant is then robustly stabilized against coprime factor uncertainty; formulae for the controller (say K) are given by McFarlane and Glover [1990,1992]. The weights W_1 and W_2 finally form part of the controller.

Inclusion of the Elliptic filter into this design framework is straightforward as it is simply made part of the weighting function W_2. The sensor measurements will therefore filter through W_2 before progressing further through the loop. The high frequency bending modes sensed by the sensors will be filtered out at this stage. The above procedure was followed and a controller designed using the adjusted discrete filter of section 3. The implementation of Fig. 6 is based on this design. The weight W_1 and the controller K are both implemented inside the *Discrete Controller* block, while the weight W_2 which in fact is just the adjusted Elliptic filter, runs inside the *Discrete Filter* block.

A 15 Hz sinusoidal signal of constant amplitude (0.5 deg) is added to the reference input to check for the attenuation performance of the filter. This simulation does not capture the control system–structure interaction but only serves to check the stability of the closed loop system, and the attenuation characteristics of the filter.

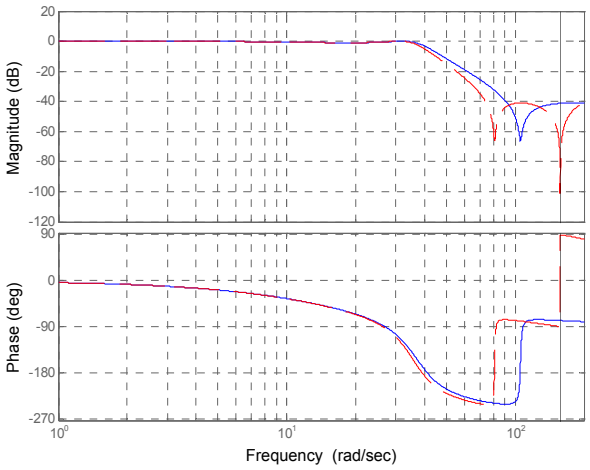

Fig. 4. Frequency Response: Analog and Discrete Elliptic filters.

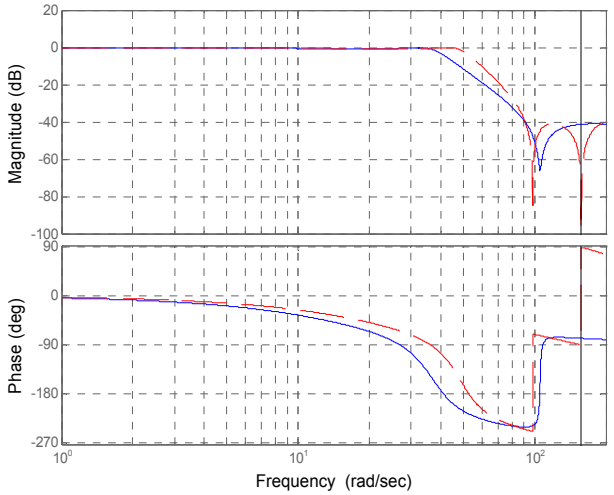

Fig. 5. Frequency Response: Analog Elliptic filter and Adjusted Discrete Elliptic filter.

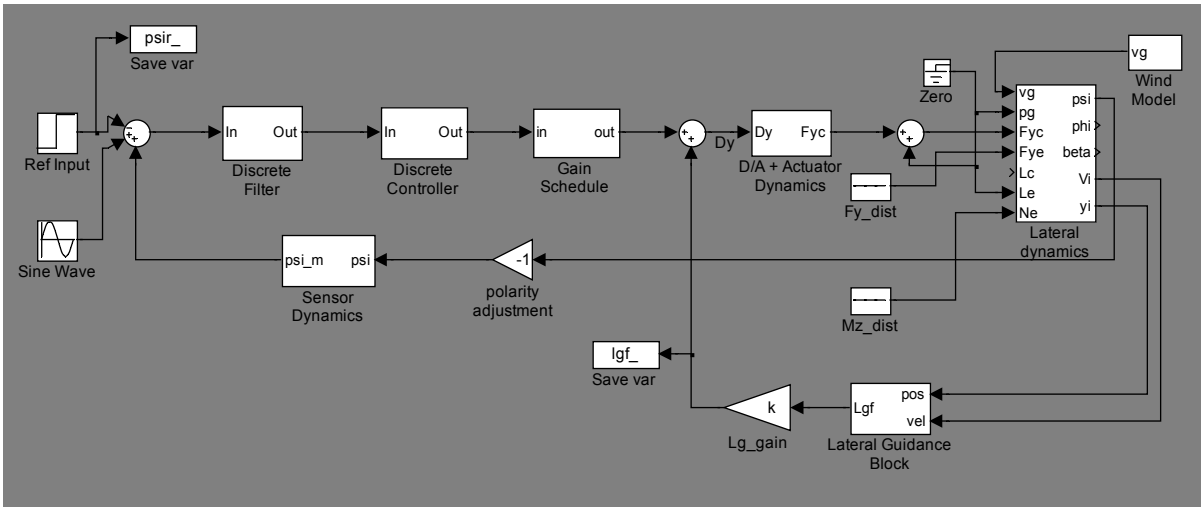

Fig. 6. Closed-loop simulation block diagram: Lateral-Directional Control.

Fig. 7 shows the reference (solid) and actual (dashed) yaw angles and the corresponding actuator commands without the filter. The high frequency is amplified and applied to the actuator. This is highly undesirable since it can cause the actuator to get damaged, and can also give rise to unstable control–structure coupling. This latter effect is not modelled in the simulation because the mode shape/slope information for the vehicle is not available; the only information available is on the lower bound of the first bending mode. The simulation is re-run with the filter in the loop and the attenuation characteristics of the filter are clearly seen from Fig. 8. The actuator signal is greatly improved.

5. APPLICATION: FLIGHT TEST RESULTS

Here two flight test results of an experimental sounding rocket (Fig. 9) are presented. This vehicle can carry payloads to altitudes in excess of 130 km. The first flight of the vehicle was carried out with no consideration of flexible dynamics in the control system design. Figs. 10 and 11 show the telemetred values of pitch and yaw error angles for this flight (when no body bending filter was employed). The corresponding actuator deflections are also shown in these figures. The structure–control system coupling is apparent. The body bending mode is excited, and the actuators respond to the structural vibrations amplifying the mode (positive feedback). This is clear from the initial portion (the first 5 seconds) of the figures. The limit on the actuator deflection causes the system oscillation to remain bounded; otherwise the controller—structure coupling could have proven destructive. The simulation results shown in the previous section did not include this effect, but this is clearly indicated in the flight test results.

The next flight was conducted with the adjusted discrete Elliptic filter in the loop to filter the high frequency

oscillations. The telemetred results of this flight are shown in Figs. 12 and 13. Fig. 12 shows the pitch error angle along with corresponding actuator deflection and Fig. 13 shows the yaw angle and the yaw actuator deflection. It is clear that the body bending mode is gain stabilized (filtered out).

6. CONCLUSION

In conclusion, it can be said that 3rd order Elliptic filters can provide satisfactory gain stabilization for flexible vehicles. One does not need to know the detailed modal response of the vehicle structure, but only an estimate on the lower bound of the first modal frequency.

However, the closed-loop bandwidth must be small enough so that the phase lag of the filter does not significantly deteriorate the closed-loop stability. It is seen that the steeper roll off and better phase characteristics of the Elliptic filter makes it well-suited for such applications.

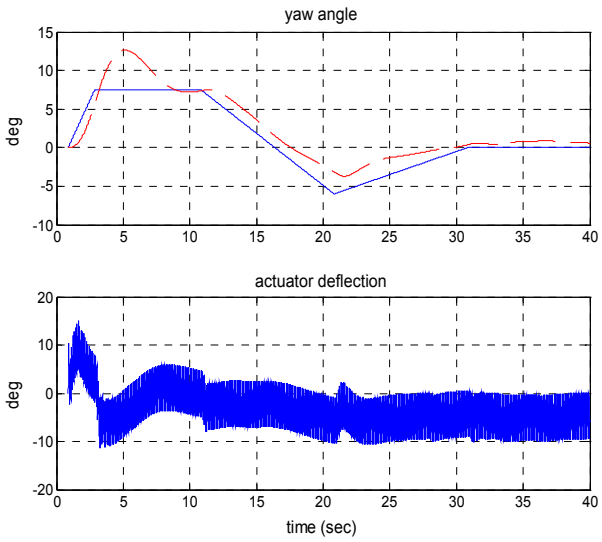

Fig. 7. Closed-loop Simulation: Yaw angle tracking and corresponding actuator deflection without filter.

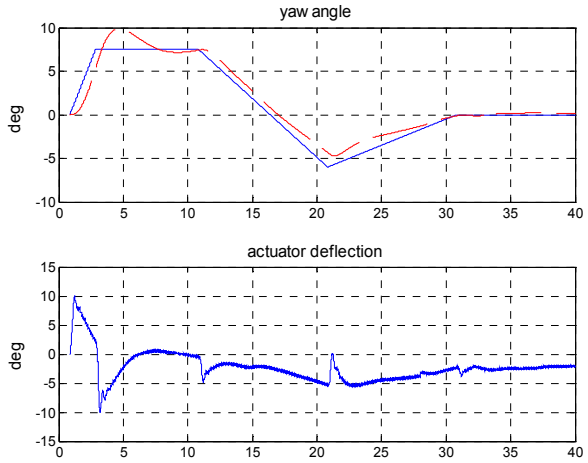

Fig. 8. Closed-loop Simulation: Yaw angle tracking and corresponding actuator deflection with filter.

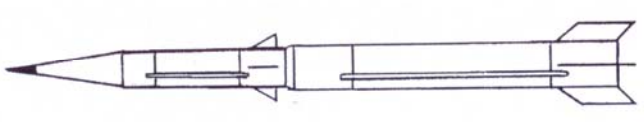

Fig. 9. Line drawing of the experimental sounding rocket.

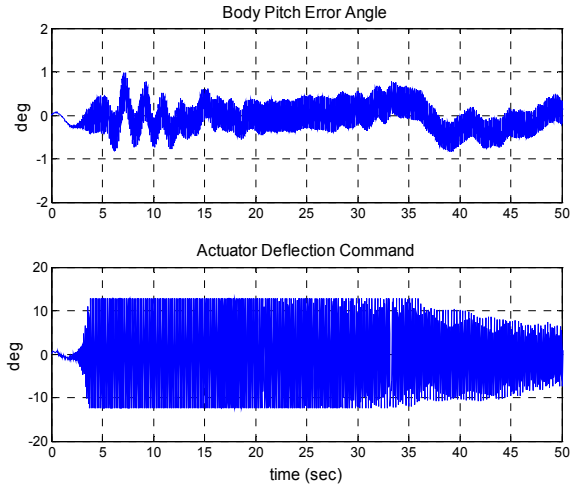

Fig. 10. Flight Test 1: Pitch error angle and corresponding actuator deflection without filter.

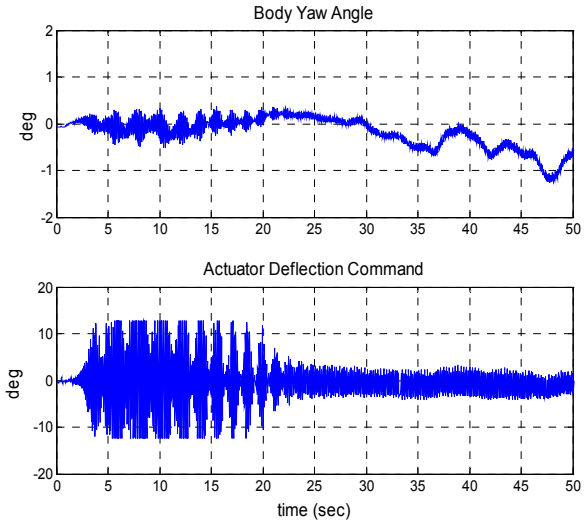

Fig. 11. Flight Test 1: Yaw angle tracking and corresponding actuator deflection without filter.

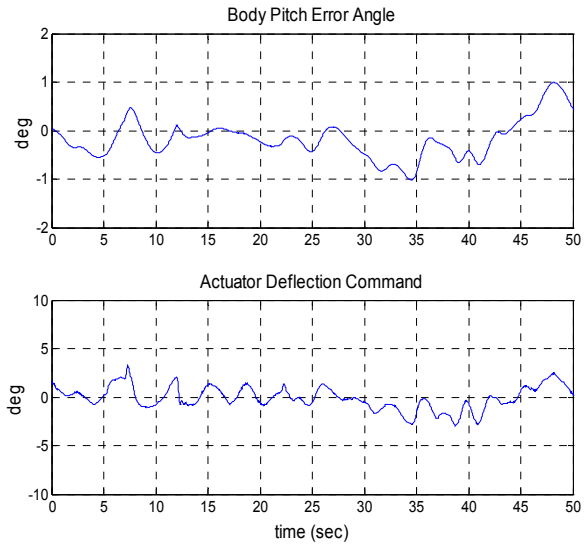

Fig. 12. Flight Test 2: Pitch error angle and corresponding actuator deflection with filter.

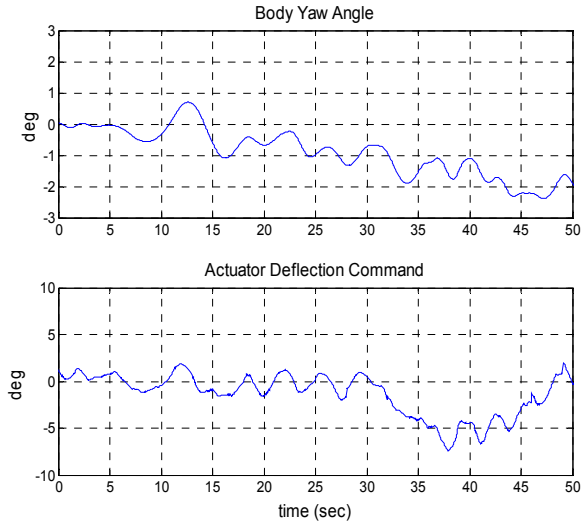

Fig. 13. Flight Test 2: Yaw angle tracking and corresponding actuator deflection with filter.

REFERENCES

Antoniou, A. (1993). *Digital filters: analysis, design, and applications*. Second Edition, McGraw-Hill.

Blakelock, J.H. (1991). *Automatic control of aircraft and missiles*. John Willey & Sons Inc., USA.

Chang, I.S., S. Toda and S. Kibe (2000). European space launch failures. In: *36th AIAA/ASME/SAE/ASEE Joint Propulsion Conference and Exhibit*, Alabama, USA.

Chirlian, P.M. (1994). *Signals and filters*. Van Nostrand Reinhold.

Dotson, K.W., R.L. Baker and B.H. Sako (1998). Launch vehicle self-sustained oscillation from aeroelastic coupling part 1: theory. *Journal of Spacecraft and Rockets*, **35**(3):365—373.

Franklin, G.F., J.D. Powell and M. Workman (1998). *Digital control of dynamic systems*. 3rd Edition, Addison-Wesley, USA.

Idan, M., M. Karpel and B. Moulin (1999). Aeroservoelastic interaction between aircraft structural and control design schemes. *Journal of Guidance, Control and Dynamics*, **22**(4):513—519.

Jackson, L. (1996). *Digital filtering and signal processing with MATLAB exercises*. Third Edition, Kluwer Academic Publishers.

Lapsley, P., J. Bier, A. Sholam and E.A. Lee (1997). *DSP processor fundamentals: architectures and features*. IEEE Press.

Livet, T., F. Kubica and J.F. Magni (1995). Robust flight control design with respect to delays, control efficiencies and flexible modes. *Control Engineering Practice*, **3**(10):1373—1384.

Mathworks. (1999). *Signal processing toolbox user's guide.* The Mathworks, Inc., USA.

Mathworks. (2001). *Filter design toolbox user's guide.* The Mathworks, Inc., USA.

McFarlane D.C. and K. Glover (1990). *Robust controller design using normalized coprime factor plant descriptions*, **volume 138 of** *Lecture Notes in Control and Information Sciences*. Springer-Verlag, Berlin.

McFarlane, D. and K. Glover (1992). A loop shaping design procedure using H∞ synthesis. *IEEE Transactions on Automatic Control,* **37**(6):759—769.

Mitra, S. K. (1998). *Digital signal processing: a computer-based approach*. McGraw-Hill.

Noll, R.B., J. Zvara and J.J. Deyst (1970). *Effects of structural flexibility on launch vehicle control systems (NASA SP-8036),* NASA, USA.

Noll, R.B. and J. Zvara (1971). *Structural interaction with control systems (NASA SP-8079),* NASA, USA.

Oppenheim, A.V. and R.W. Schafer (1989). *Discrete-time signal processing*. Prentice-Hall.

Samar, R., G. Murad, I. Postelthwaite and D.-W. Gu (1996). A discrete-time H_∞ observer-based controller and its application to a glass tube production process. *European Journal of Control,* **2**:112—125.

Skogestad, S. and I. Postlethwaite (2005). *Multivariable Feedback Control Analysis and Design*. Second Edition, John Wiley & Sons.

Smerlas, A., D.J. Walker, I. Postelthwaite, M.E. Strange, J. Howitt and A.W. Gubbells (2001). Evaluating H_∞ controllers on the NRC Bell 205 fly-by-wire helicopter. *Control Engineering Practice,* **9**(1):1—10.

Tsai, M.C., E.J.M. Geddes and I. Postlethwaite (1992). Pole-zero cancellations and closed-loop properties of an H_∞ mixed sensitivity design problem. *Automatica,* **28**(3):519—530.